UNIVERSIDADE TECNOLÓGICA FEDERAL DO PARANÁ
PROGRAMA DE PÓS-GRADUAÇÃO EM ENGENHARIA ELÉTRICA

JOÃO GUILHERME RAMINELLI

PLATAFORMA DE TESTES DINÂMICOS PARA AMORTECEDORES MAGNETO-REOLÓGICOS E REPRESENTAÇÃO ATRAVÉS DE MODELOS DE HISTERESE

DISSERTAÇÃO

CORNÉLIO PROCÓPIO

2020

JOÃO GUILHERME RAMINELLI

PLATAFORMA DE TESTES DINÂMICOS PARA AMORTECEDORES MAGNETO-REOLÓGICOS E REPRESENTAÇÃO ATRAVÉS DE MODELOS DE HISTERESE

DYNAMIC TEST PLATFORM FOR MAGNETOLOGICAL DAMPER AND REPRESENTATION THROUGH HYSTERESIS MODELS

Dissertação apresentada como requisito para obtenção do título de Mestre em Engenharia Elétrica da Universidade Tecnológica Federal do Paraná (UTFPR).
Orientador: Alessandro do Nascimento Vargas.

CORNÉLIO PROCÓPIO

2020

TERMO DE APROVAÇÃO

Título da Dissertação Nº 066:

"Plataforma de Testes Dinâmicos para Amortecedores Magneto-reológicos e Representação através de Modelos de Histerese".

por

João Guilherme Raminelli

Orientador: Prof. Dr. Alessandro do Nascimento Vargas

Esta dissertação foi apresentada como requisito parcial à obtenção do grau de MESTRE EM ENGENHARIA ELÉTRICA – Área de Concentração: Sistemas Eletrônicos Industriais, pelo Programa de Pós-Graduação em Engenharia Elétrica – PPGEE – da Universidade Tecnológica Federal do Paraná – UTFPR – Câmpus Cornélio Procópio, às 09h00 do dia 19 de outubro de 2020. O trabalho foi _____ pela Banca Examinadora, composta pelos professores:

Prof. Dr. Alessandro do Nascimento Vargas
Presidente

Prof. Dr. Aldemir Aparecido Cavalini Júnior
UFU

Prof. Dr. Marcio Aurélio Furtado Montezuma
UTFPR-CP

Visto da coordenação:

Prof. Dr. Leonardo Poltronieri Sampaio
Coordenador do Programa de Pós-Graduação em Engenharia Elétrica
UTFPR Câmpus Cornélio Procópio

A Folha de Aprovação assinada encontra-se na Coordenação do Programa.

SUMÁRIO

AGRADECIMENTOS

Quero agradecer a Deus, em primeiro lugar, pela força e coragem ao longo desta jornada.

Aos professores do programa, especialmente o professor Marcio Aurelio Furtado Montezuma por todo o conhecimento compartilhado, o qual tornou possível a realização desta pesquisa.

Ao meu orientador, Alessandro do Nascinamento Vargas, por todo incentivo ao meu desenvolvimento e pela paciência na orientação. Seu direcionamento foi fundamental para o sucesso desta dissertação.

Agradeço meus pais e minha esposa Daniele, que com muito afeto me apoiaram nessa fase da minha vida.

Aos meus amigos e colegas, por seu incentivo e apoio constantes.

Agradeço à UTFPR pelo apoio financeiro durante os seis primeiros meses de pesquisa, bem como por toda infraestrutura disponibilizada para a realização da mesma.

O presente trabalho foi realizado com apoio da Coordenação de Aperfeiçoamento de Pessoal de Nível Superior - Brasil (CAPES) - Código de Financiamento 001.

”Concentre todos seus pensamentos na tarefa que está realizando. Os raios de sol não queimam até que sejam colocados em foco.” - Alexander Graham Bell

RESUMO

RAMINELLI, João G.. PLATAFORMA DE TESTES DINÂMICOS PARA AMORTECEDORES MAGNETO-REOLÓGICOS E REPRESENTAÇÃO ATRAVÉS DE MODELOS DE HISTERESE . f. Dissertação – Programa de Pós-graduação em Engenharia Elétrica, Universidade Tecnológica Federal do Paraná. Cornélio Procópio, 2020.

O amortecedor mecânico é um dispositivo usado de maneira geral na proteção do sistema ao qual está acoplado, visando minimizar os efeitos de vibrações que possam causar danos.

Os amortecedores podem ser classificados em três formas: amortecedores passivos, amortecedores ativos e amortecedores semiativos. Neste último tipo temos amortecedores que usam fluído magneto-reológico, e eles têm atraído a atenção de pesquisadores pela alta confiabilidade e custo modesto.

Os fluídos magneto-reológicos podem modificar suas propriedades mecânicas por meio de sinal de controle. Entretanto conhecer a dinâmica deste tipo de dispositivo é uma tarefa difícil devido ao comportamento histerético que este apresenta.

Para obter os dados experimentais mostrados nessa dissertação, foi construída uma plataforma de ensaios na qual o amortecedor magneto-reológico é acoplado a uma mesa e excitado com diferentes frequências e deslocamentos.

Os dados obtidos foram utilizados para calcular os parâmetros de um modelo matemático, conhecido como modelo de Dahl, capaz de descrever o comportamento de histerese do amortecedor.

O modelo de Dahl foi usado neste trabalho em associação a um modelo de estrutura de edifício de dois andares. O objetivo foi avaliar o comportamento da estrutura do prédio quando sujeitado a um terremoto. Essa simulação indica que o uso de amortecedor MR em estruturas é capaz de minimizar os danos físicos causados a estrutura por um eventual terremoto.

Palavras-chave: Dispositivo mecânico, Vibrações, Histerese, Bouc-wen, Dahl, Amortecedores.

ABSTRACT

RAMINELLI, João G.. DYNAMIC TEST PLATFORM FOR MAGNETOLOGICAL DAMPER AND REPRESENTATION THROUGH HYSTERESIS MODELS. f. Dissertação – Programa de Pós-graduação em Engenharia Elétrica, Universidade Tecnológica Federal do Paraná. Cornélio Procópio, 2020.

The mechanical damper is a device generally used to protect the system to which it is attached, to minimize the effects of vibrations that may cause damage.

Dampers can be classified into three forms: passive dampers, active dampers, and semi-active dampers. In the latter type, we have shock absorbers that use magneto-rheological fluid, and they have attracted the attention of researchers due to their high reliability and modest cost.

Magneto-rheological fluids can modify their mechanical properties using a control signal. However, knowing the dynamics of this type of device is a difficult task due to its hysterical behavior.

To obtain the experimental data shown in this dissertation, a test platform was built in which the magneto-rheological damper is coupled to a table and excited with different frequencies and displacements.

The data obtained were used to calculate the parameters of a mathematical model, known as the Dahl model, capable of describing the hysteresis behavior of the shock absorber.

The Dahl model was used in this work in association with a two-story building structure model. The objective was to assess the behavior of the building's structure when subjected to an earthquake. This simulation indicates that the use of MR shock absorber in structures can minimize the physical damage caused to the structure by an eventual earthquake.

Keywords: Mechanical device, Vibrations, Hysteresis, Bouc-wen, Dahl, Dampers.

1 INTRODUÇÃO

O amortecedor mecânico é um dispositivo usado de maneira geral na proteção do sistema ao qual está acoplado, visando minimizar os efeitos de vibrações que possam causar danos. Esses dispositivos são aplicados nas mais diversas áreas, como construção civil (AGUIRRE et al., 2010b), suspensão veicular (STUTZ, 2005), próteses médicas (GAO et al., 2017) e estabilizar instrumentos de precisão (MENG et al., 2019).

Os amortecedores podem ser classificados em três formas. Amortecedores passivos são aqueles que funcionam em uma faixa de trabalho restrita, não são adaptados às diferentes condições de operação e seu projeto é específico para atender as demandas do sistema que ele será acoplado (LIMA, 2011).

Os amortecedores ativos são capazes de injetar energia no sistema para controlá-lo, entretanto, necessitam de uma fonte de energia externa. Tais amortecedores podem ser pneumáticos, hidráulicos ou eletromagnéticos, e geralmente possuem maior custo de implementação e manutenção quando comparados aos amortecedores passivos. Um ponto negativo dos amortecedores ativos é que possuem dependência de uma fonte de energia externa para atuar (STUTZ, 2005).

Os amortecedores semiativos não podem injetar energia no sistema, mas podem controlar a dissipação de energia ajustando suas propriedades mecânicas em tempo real por meio de um sinal de controle, o que geralmente lhes confere um baixo consumo de energia. Em caso de falta de energia, o dispositivo funciona passivamente, tornando seu uso relativamente confiável (LIMA, 2011). Cilindros com vazão controlável, hidráulicos ou pneumáticos (KONIECZNY et al., 2006), (FARAJ et al., 2018) e amortecedores de fluidos controláveis, como fluido magneto-reológico, são exemplos de dispositivos semiativos (STUTZ, 2005).

Amortecedores que usam fluído magneto-reológico têm atraído a atenção de pesquisadores pela alta confiabilidade e custo modesto (DYKE et al., 1999). Os fluídos magneto-reológicos podem modificar suas propriedades mecânicas para lidar com a vari-

ação das grandezas físicas as quais são submetidos, como temperatura, pressão, campo magnético (YANG et al., 2002). Desta forma, estes amortecedores são utilizados em diversos sistemas mecânicos tais como suspensões automotivas, sistemas de amortecimento sísmico e próteses inteligentes(ROSSI et al., 1999),(LIMA, 2011). Entretanto conhecer a dinâmica deste tipo de dispositivo é uma tarefa difícil devido ao comportamento histerético que este apresenta (PONS, 2005), (ZAMANI et al., 2019). Este trabalho gera contribuição no tocante de entender melhor o funcionamento de amortecedor magneto-reológico (MR) determinando o seu comportamento dinâmico baseado em dados experimentais. Além disso, o modelo desenvolvido aqui é usado para determinar a capacidade do amortecedor MR em atenuar vibrações em um estrutura de dois andares.

Para obter os dados experimentais mostrados nessa dissertação, foi construída uma plataforma de ensaios na qual o amortecedor MR é acoplado a uma mesa e excitado com diferentes frequências e deslocamentos. Os dados obtidos foram utilizados para calcular os parâmetros de um modelo matemático capaz de descrever o comportamento de histerese do amortecedor.

O modelo de histerese adotado nessa dissertação é conhecido como modelo de Dahl. Em 1968, P. R. Dahl modelou a força de atrito como uma função do deslocamento relativo de duas superfícies de contato para o Centro de Sistemas Espaciais e Mísseis dos Estados Unidos. (DAHL, 1968). O modelo de Dahl é um caso particular do modelo de Bouc-Wen. O modelo de Bouc-Wen é tradicionalmente usado para representar histerese, mas apresenta parâmetros excessivos quando a tarefa em questão é descrever apenas a relação entre deslocamento e força restauradora (IKHOUANE; RODELLAR, 2007). Desta forma, a literatura sugere o modelo de Dahl como uma alternativa mais simples em relação ao modelo de Bouc-Wen. Para o cálculo dos parâmetros do modelo de Dahl mostrado nessa monografia, foi utilizada a metodologia apresentada por (IKHOUANE; RODELLAR, 2007). Em resumo, o modelo de Dahl foi usado para representar um amortecedor MR.

O modelo de Dahl, representando um amortecedor MR, foi acoplado a um modelo de estrutura de edifício de dois andares. O objetivo foi avaliar o comportamento da estrutura do edificio quando sujeitado a um terremoto em três diferentes cenários, ou seja, estrutura sob terremoto (i) sem a proteção do amortecedor MR, (ii) com a proteção do amortecedor MR sem tensão aplicada a ele, e (iii) com a proteção do amortecedor MR com tensão aplidada a ele. Nota-se, na simulação, que o caso (iii) foi aquele capaz

de promover a maior atenuação das vibrações causadas por terremoto. Essa simulação indica que o uso de amortecedor MR em estruturas é capaz de minimizar os danos físicos causados a estrutura por um eventual terremoto.

2 THEORY OF SYSTEMS WITH HYSTERESIS

The aim of the present chapter is twofold. First, this chapter recalls a nonlinear model useful for describing the hysteresis behavior. Second, this chapter shows a procedure to determine the parameters of that model.

2.1 HYSTERESIS

Hysteresis is a nonlinear behavior in which the system state depends on the history of the state, together with memory effects. Hysteresis can be found in several devices, such as in steering and suspension of vehicles (DUTTA; CHOI, 2018), in construction of structures (ZAPATEIRO et al., 2009), in nanopositioning stages (SALAPAKA et al., 2002), in adaptive structural shape control (ANDERSON et al., 1992), in structural health monitoring (INMAN; CARNEIRO, 2020), in acoustic systems (SARNO; FRANKE, 1994), in hybrid transducers (GE; JOUANEH, 1995), among other applications (ISMAIL et al., 2009). For mechanical and structural systems, in particular, hysteresis denotes the memory of inelastic behavior in which the restorative force acts against the force imposed by the dissipating energy. The restorative force depends not only on instantaneous deformation but also on the past deformation (ISMAIL et al., 2009).

Using the laws of physics to model hysteresis in devices becomes a complicated task, (ISMAIL et al., 2009). The difficulty arises because certain hysteresis processes require complex models, and often internal variables are non-measurable, making difficult the model validation (NOËL et al., 2016), (AGUIRRE et al., 2010a).

As an attempt to overcome these modeling difficulties, some authors have developed simple models that account for the hysteresis through a semi-physical modeling known as the Bouc-Wen model, (ISMAIL et al., 2009) as described next.

2.2 THE BOUC-WEN MODEL

The Bouc-Wen (BW) model was introduced in the '70s (BOUC, 1971), (WEN, 1976), and since then, it has been used to describe the hysteretic behavior of various devices (ISMAIL et al., 2009). The BW model can be interpreted as a mechanical system containing three elements (SPENCER et al., 1997): spring, damper, and hysteresis term, as presented in Figure 2.1. Note that the BW model relates displacement to restoration force using a first-order nonlinear differential equation.

The force generated by this three-element mechanical system is given by

$$F(t) = c_0\dot{x}(t) + k_0(x(t) - x_0) + \alpha\dot{z}(t), \tag{2.1}$$

where c_0 is the damping coefficient, k_0 is the linear spring parameter, x_0 is the initial spring displacement, and α is the Bouc-Wen parameter coefficient associated with the hysteretic component z that satisfies (ISMAIL et al., 2009)

$$\dot{z}(t) = -\gamma z(t)|\dot{x}(t)||z(t)|^{n-1} - \beta\dot{x}(t)|z(t)|^n + A\dot{x}(t). \tag{2.2}$$

The parameters α, β, γ, A, and n should be adjusted to represent the hysteretic behavior of the process under study. The Bouc-Wen model is then a single-input single-output model able to describe processes subject to hysteresis. When experimental data taken from a process with hysteresis is available, one can use this data to identify the parameters α, β, γ, A, and n. Figure 2.2 shows an example in which the Bouc-Wen model generates the hysteretic loop.

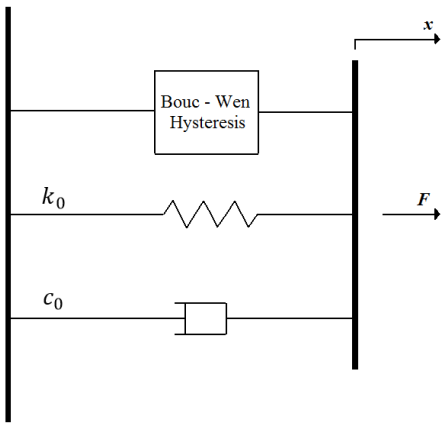

Figure 2.1: Bouc-Wen model of magnetorheological damper.

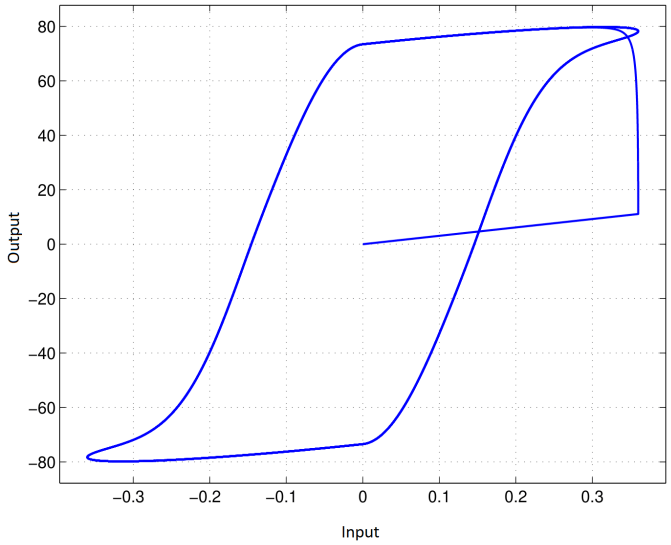

Figure 2.2: Phase portrait of the Bouc-Wen model in (2.2) with $\alpha = 0.1$, $\beta = 0.1$, $\gamma = 2$, $A = 1$ and $n = 1.3$.

2.2.1 THE DAHL MODEL

It is known that the BW model has excessive parameters when the task at hand is to describe the relationship between displacement and restorative force (IKHOUANE; RODELLAR, 2007). The literature then suggests a simplified version of the BW model, known as the Dahl model, which is given by (PIATKOWSKI, 2014)

$$F(t) = k_x[v(t)]\dot{x}(t) + k_w[v(t)]w(t), \tag{2.3}$$

$$\dot{w}(t) = \rho(\dot{x}(t) - |\dot{x}(t)|w(t)), \tag{2.4}$$

where $\dot{x}(t)$ denotes the damper piston velocity, $v(t)$ denotes the voltage input command of the amplifier, $F(t)$ represents the damping force, and $w(t)$ describes the nonlinear behavior of the damper. The viscous friction coefficient k_x, the dry friction coefficient k_w, and the parameter ρ may depend on the voltage $v(t)$ (AGUIRRE et al., 2010a).

Next section recalls a procedure used to identify the parameters of the Dahl model in (2.3) and (2.4).

2.3 IDENTIFICATION OF THE DAHL MODEL

The identification procedure described next is available in (IKHOUANE; RODELLAR, 2007). The procedure assumes the knowledge of the hysteresis loop $(\bar{F}(\tau), x(\tau))$ parameterized with the variable $\tau \in [0, T^+]$. Recalling that $x(\tau)$ represents the system input and $F(\tau)$ represents the system output, the constant k_x of the system can be determined as follows

$$k_x = \frac{\bar{F}(0) + \bar{F}(T^+)}{\dot{x}(0) + \dot{x}(T^+)}. \tag{2.5}$$

Here the terms $\bar{F}(0)$, $\bar{F}(T^+)$, $\dot{x}(0)$, and $\dot{x}(T^+)$ correspond, respectively, to the damping force and speed when the damper reaches the minimum $x(0)$ and maximum $x(T^+)$ displacements.

In practice, the input signal should be selected in a way that avoids division by zero in the denominator of (2.5). Using k_x from equation (2.5), the quantity $k_w\bar{w}(t)$ can be computed from

$$\theta(\tau) = k_w\bar{w}(\tau) = \bar{F}(\tau) - k_x\dot{x}(\tau). \tag{2.6}$$

The function $\theta(\tau)$ is key for calculating the remaining parameters of the Dahl model, as described next. The parameter a is determined as follows

$$a = \left[\frac{d\theta(x)}{dx}\right]_{x=x_*}, \tag{2.7}$$

where x_* is some value that satisfies the relation $\theta(x_*) = 0$. Now, taking some value $x_{*1} > x_*$, the parameter ρ can be determined from the expression

$$\rho = \frac{a - \left[\frac{d\theta(x)}{dx}\right]_{x=x_{*1}}}{\theta(x_{*1})}. \tag{2.8}$$

Finally, the parameter k_w is defined as follows

$$k_w = \frac{a}{\rho}. \tag{2.9}$$

2.4 NUMERICAL EXAMPLE

This section's aim is to illustrate the identification method of the parameters considered by the Dahl model.

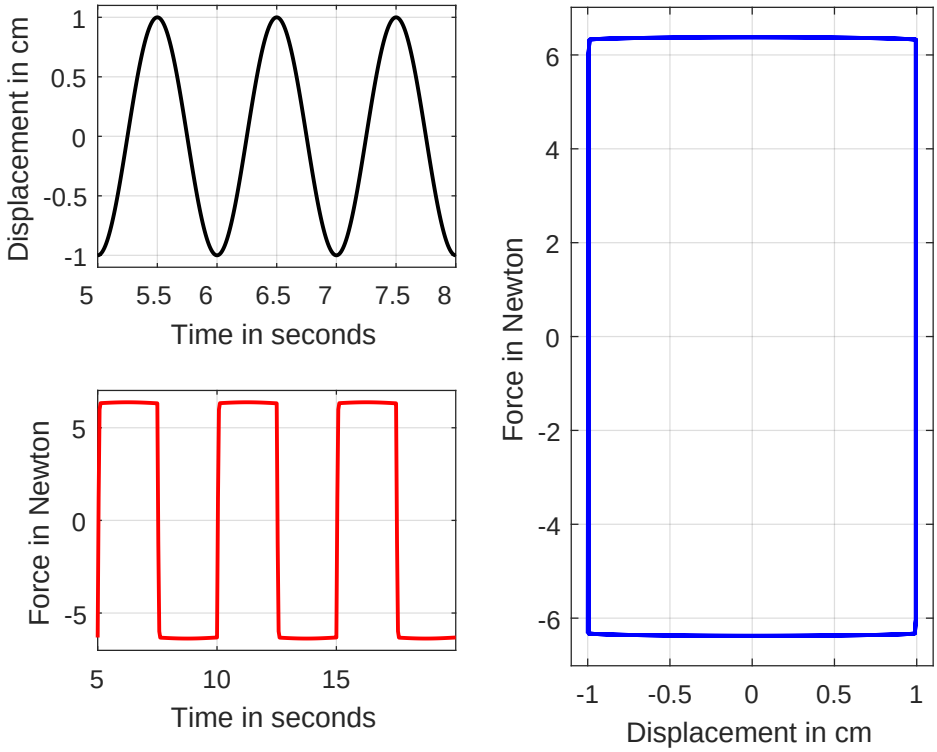

Figure 2.3: Response of the MR damper model.

Step 1

Consider the Dahl model in equations (2.3) and (2.4) with $k_x = 0.045$, $k_w = 6.32$ and $\rho = 705.32$. This model was evaluated under a periodic displacement with an amplitude of $0.8\,cm$ and a frequency of $0.2\,Hz$. Figure 2.3 shows the displacement (input) and the corresponding force (output).

Step 2

From the data, we obtained $\bar{F}(0) = -6.3199N$, $\bar{F}(T^+) = 6.3200N$, $\dot{x}(0) = 7.8957 * 10^{-5}$, and $\dot{x}(T^+) = 2.3687 * 10^{-4}$. Thus

$$k_x = 0.045.$$

This value coincides with the value of k_x given in Step 1.

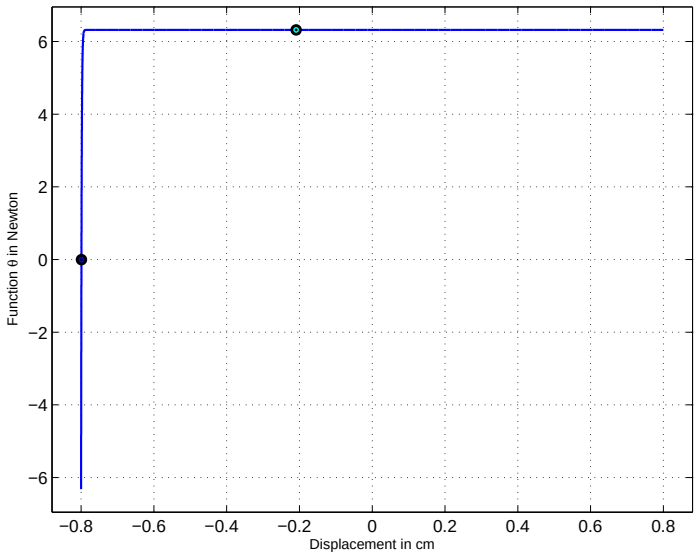

Figure 2.4: Function θ with x_* in black and x_{*1} in green.

Step 3

The θ function is shown in Figure 2.4. As can be seen, the point x_* in which the function $\theta(x_*)$ reaches zero is close to $x_* = -0.8\,cm$.

Step 4

The value of the parameter a is calculated by equation (2.7), which requires the function $\theta(x_*)$ to extract the function derivative in which x_* satisfies the relation $\theta(x_*) = 0$. The data yield

$$a = 4466.3\,N/cm.$$

Step 5

The value $x_{*1} = -0.2092$ is chosen arbitrarily, resulting in

$$\rho = 706.687\,cm^{-1} \quad \text{and} \quad k_w = 6.32\,N.$$

3 STRUCTURE AND CONSTRUCTION

Dampers are devices used to vibration attenuation purposes in mechanical systems and are capable of dissipating energy from the system in which they are connected. Most dampers have fixed dissipation properties; however, magnetorheological (MR) dampers present dissipation properties that can be controlled. Controlling the dissipation properties of a damper expands its usefulness in engineering (ROSSI et al., 1999), (LIMA, 2011), (CHEN et al., 2016), (SEID et al., 2018), (DO et al., 2016).

Due to their advantages, such as high reliability and modest cost of implementation (DYKE et al., 1999), MR dampers have been used in the most diverse mechanical systems such as automotive suspensions, seismic damping systems, and smart prostheses (ROSSI et al., 1999), (LIMA, 2011). However, for the correct application of this technology, it is necessary to understand its nonlinear behavior (PONS, 2005).

To improve our understanding of MR dampers, we decided to construct a laboratory testbed, which was assembled to verify the behavior of an industrial magnetorheological damper. In the experiments, the selected device was the model RD-8041-1 manufactured by LORD Corporation, USA. The MR damper was connected to a carefully designed mechanical structure, as described next.

The mechanical structure was able to excite the damper with different combinations of displacements and frequencies, and an electronic circuitry was responsible for measuring and recording the corresponding data. The experimental goal was to generate data that allowed us to model the MR damper. For the modeling, we have considered the Dahl model. The mechanical structure can create distinct patterns of vibrations, for instance, by emulating earthquakes in tiny structures.

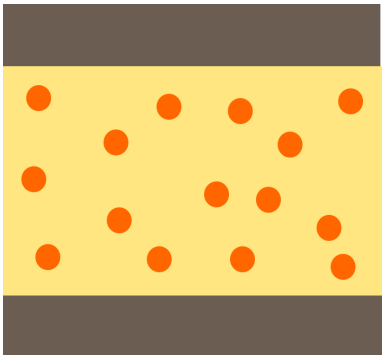

Figure 3.1: MR fluid in the absence of a magnetic field.

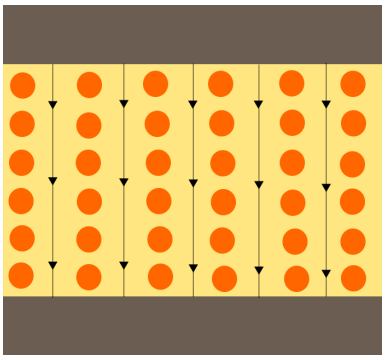

Figure 3.2: MR fluid in the presence of a magnetic field.

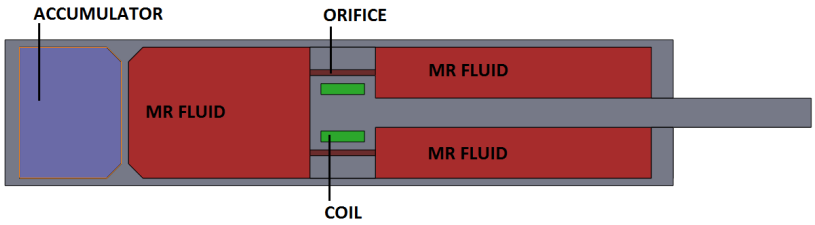

Figure 3.3: MR Fluid-based Damper.

3.1 STRUCTURE

Magnetorheological (MR) dampers use fluids that contain large amounts of small, highly magnetizable particles (VICENTE et al., 2011). These fluids have less shear resistance, a lower working temperature, and high energy dissipation capacity (YARALI et al., 2019). The MR properties of the fluid depend on the particle shape distribution, particle concentration, carrier fluid properties, temperature, and applied magnetic field (JOLLY et al., 2012).

When a magnetic field is applied in the fluid, the particles align themselves

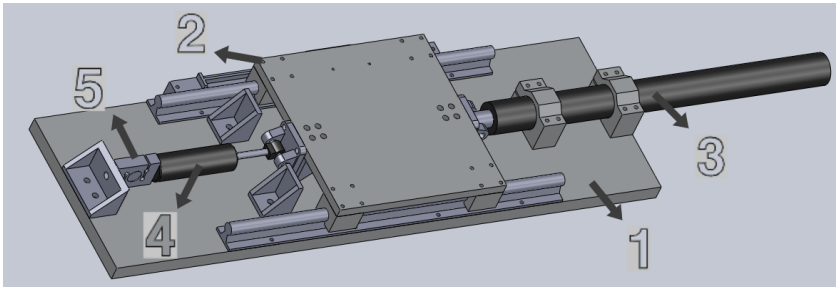

Figure 3.4: Proposed shaking table connected with a magnetorheological damper.

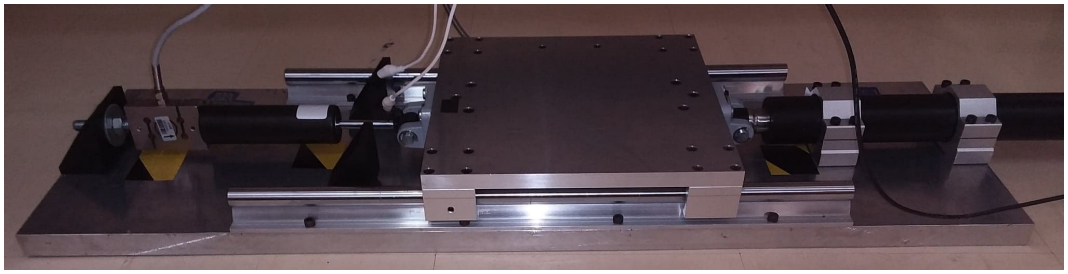

Figure 3.5: Laboratory testbed.

due to a dipolar moment, which is parallel to the direction of the field flow lines. The alignment of these particles forms a current-like structure, as shown in Figures 3.1 and 3.2.

Once the particles are aligned, they become more resistant to any force that tries to move them. The fluid's resistance, which depends on the amount of aligned particles, is proportional to the magnetic field intensity. This rearrangement of the particles occurs within milliseconds and affects the fluid's viscosity almost immediately. Due to this feature, MR fluid can be used in applications that require an immediate change of the fluid viscosity. In particular, MR fluid has been applied to dampers to mitigate vibrations (LIMA, 2011), (ISMAIL et al., 2009).

Figure 3.3 shows the components of an MR damper. The main damper cylinder contains the piston, the magnetic circuit (coil), the accumulator, and the magnetorheological fluid. When the damper extends, the piston forces the MR fluid to pass through the valve, making the fluid move from one chamber to another. By controlling the magnetic field's intensity, one controls the resistance of the fluid that flows through the valve, resulting in the control of the resistance of the piston against movements (CARLSON; JOLLY, 2000).

3.2 EXPERIMENTAL SETUP: PRACTICAL ASPECTS

Figure 3.4 shows the main device assembled in the laboratory. It works as a single-axis shaking table. It is composed of a metal-solid base [1] with a sliding table [2] over it. At one end, an actuator [3] is attached to the sliding table for producing displacements. At the other end, the MR damper [4] is attached. The MR damper is attached to a load cell [5], which measures the force. This setup allowed us to capture information such as displacement and force that are essential for calculating

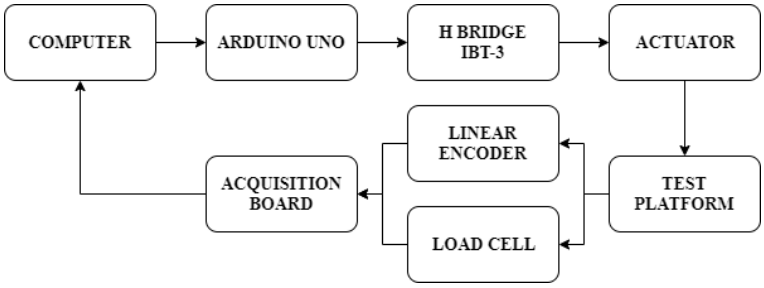

Figure 3.6: Electronic block diagram.

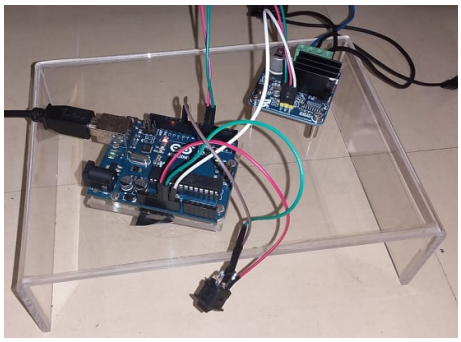

Figure 3.7: Arduino Uno and IBT-3 Drive.

the parameters of the Dahl model. The experimental setup is shown in Figure 3.5.

Experimental data were measured and recorded through an electronic circuit. The electronic connection followed the block diagram of Figure 3.6. An Arduino Uno board was used to generate a PWM signal, which fed an IBT-3 Drive Module, see Figure 3.7. This module provided the energy to the actuator so that it moved forward and backward at the frequency programmed in the Arduino Uno board.

The forces applied in the MR damper were measured by the load cell model ZSL manufactured by IWM, which psent signals to the data acquisition board. Figure 3.8 shows the load cell attached to the MR damper. A linear encoder was used to measure the displacements of the rod.

3.3 RESEARCH DEVELOPMENT

According to the objectives of the work, the following steps were taken:

Step 1:

Experiments in the laboratory testbed. The MR damper was excited under

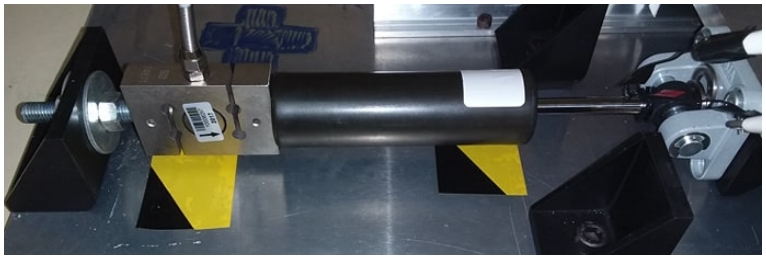

Figure 3.8: MR damper with load cell.

sine-wave displacement inputs. The sine waves considered distinct frequencies and amplitudes. The experiments were carried out with an MR damper subjected to different voltages. Each test generated data that was collected and stored, and the coefficients k_x, k_w, and ρ were calculated accordingly.

Step 2:

Accuracy of the model. We calculate the standard L^1 norm, which evaluates the difference between the force generated by the Dahl model and the force generated during the experimental tests.

$$\varepsilon = \frac{||F_e - F||_1}{||F_e||_1}, \tag{3.1}$$

where F_e denotes the experimental force and F denotes the simulated force.

Step 3:

Determine how useful is an MR damper when it is attached to buildings subject to earthquakes.

4 EXPERIMENTAL RESULTS

The purpose of this chapter is to show experimental data and the corresponding calculations used to identify the Dahl model.

4.1 THE DAHL MODEL: MODIFIED IDENTIFICATION METHODOLOGY

According to (AGUIRRE et al., 2010a), the parameter k_x kept fixed as in equation (2.5) can mislead the model's accuracy when the viscous friction is much less than the dry friction. To overcome such problem, the authors of (AGUIRRE et al., 2010a) suggest a procedure. We follow this procedure.

When the displacement is large enough, the hysteresis loop is in the plastic region, a fact that allows the approximation $\bar{w}(\tau) \simeq 1$ (AGUIRRE et al., 2010a). This approximation substituted into equation (2.4) yields

$$F(t) = k_x[v(t)]\dot{x}(t) + k_w[v(t)]. \tag{4.1}$$

An interesting feature of equation (4.1) is that it makes the force $F(t)$ be linear with respect to the velocity $\dot{x}(t)$. Note that the parameters k_x and k_w depend on $v(t)$ and they are not anymore represented by equations (2.5) and (2.9), respectively. The parameter ρ is given by equation (2.9),

$$\rho = \frac{a}{k_w[v(t)]}. \tag{4.2}$$

Note now that the coefficients k_x, k_w and ρ are voltage-dependent. In particular, they can become polynomial dependent (AGUIRRE et al., 2012).

$$k_x(v) = k_{x1} + k_{x2}v(t) + k_{x3}v(t)^2 + k_{x4}v(t)^3 \tag{4.3}$$

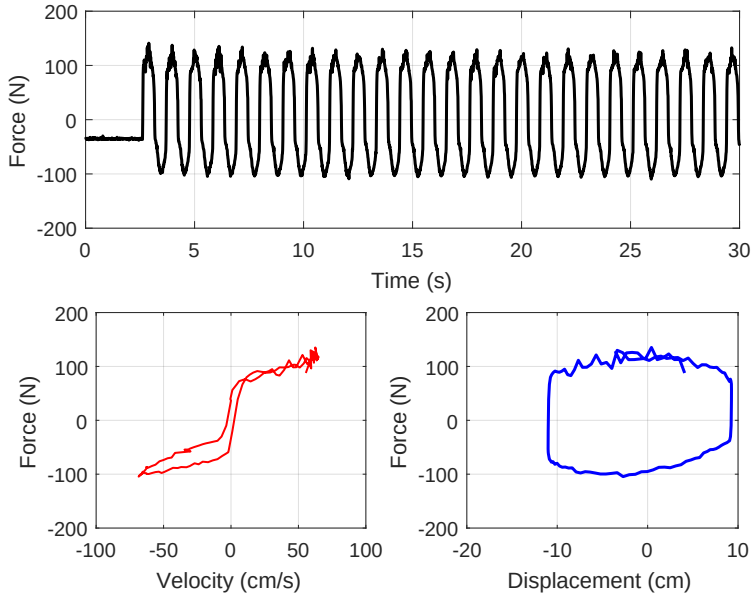

Figure 4.1: Response of the MR damper model with null voltage.

$$k_w(v) = k_{w1} + k_{w2}v(t) + k_{w3}v(t)^2 + k_{w4}v(t)^3 \tag{4.4}$$

$$\rho(v) = \rho_1 + \rho_2 v(t) + \rho_3 v(t)^2 + \rho_4 v(t)^3 \tag{4.5}$$

4.2 EXPERIMENTAL DATA: MR DAMPER WITH NULL VOLTAGE

Experiments were carried out in the laboratory testbed. No voltage was applied in the MR damper, which means that its magnetorheological fluid was demagnetized. The mechanism was programmed to excite the MR damper with displacement inputs in the form of a sine wave. A sample of the input and output data is depicted in Figure 4.1. Table 4.2 shows the amplitudes and frequencies for all sine-wave inputs. This table also shows the coefficients of the Dahl model.

The values in Table 4.2 were used to calculate the statistical mean and standard deviation of the model parameters, as given by Table 4.1.

To validate the obtained coefficients, we simulated the Dahl model in MATLAB/Simulink. The model in Simulink was excited with the same input signal used in the experimental tests. The force obtained in the model was compared to the force captured in the experiments, and the corresponding error was calculated using the L^1

Table 4.1: Calculated coefficients.

Parameter	Mean	St. Dev.
k_{xa} $(N.s.mm^{-1})$	0.8020	0.1023
k_{wa} (N)	50.2368	6.7375
ρ (mm^{-1})	42.7448	17.9213

Table 4.2: Results with null voltage.

Displacement (mm)	Frequency (Hz)	k_x $(N.s.mm^{-1})$	k_w (N)	ρ (mm^{-1})
24.75	0.8403	0.7682	57.4210	27.4527
22.81	0.8696	0.6835	59.4608	30.5753
21.72	0.8932	0.7144	56.5586	34.1413
19.96	0.9434	0.7040	53.4880	39.2073
18.26	0.9709	0.8836	48.8004	66.0383
16.63	1.0100	0.7409	49.1823	44.0407
15.16	1.0530	0.7716	50.2659	40.0764
13.65	1.0990	0.9868	38.0126	57.5001
12.28	1.1490	0.8451	46.1595	45.6716
11.24	1.2200	0.9223	43.0192	40.6709

norm. The average error from (3.1) was 14.81%.

4.3 EXPERIMENTAL DATA: MR DAMPER WITH NON-NULL VOLTAGE

Tables 4.3, 4.4, and 4.5 show the coefficients of the Dahl model when the voltages of $0.88\,V$, $1.98\,V$, and $3.21\,V$, respectively, were applied in the MR damper. Figure 4.2 shows the response of the MR damper model with $0.88\,V$.Note that the force generated by the MR damper increases when tension is applied, see Figures 4.1 and 4.2.

The values show in Tables 4.3, 4.4 and 4.5 were combined with the polynomials in (4.3)–(4.5), together with a curve-fitting procedure, to produce

$$k_x(v) = 0.0855.v(t)^3 + 0.0342.v(t)^2 + 0.4931.v(t) + 0.802, \tag{4.6}$$

$$k_w(v) = 3.6157.v(t)^3 - 24.866.v(t)^2 + 201.92.v(t) + 50.237, \tag{4.7}$$

$$\rho(v) = -2.8368.v(t)^3 + 17.881.v(t)^2 - 39.038.v(t) + 42.745. \tag{4.8}$$

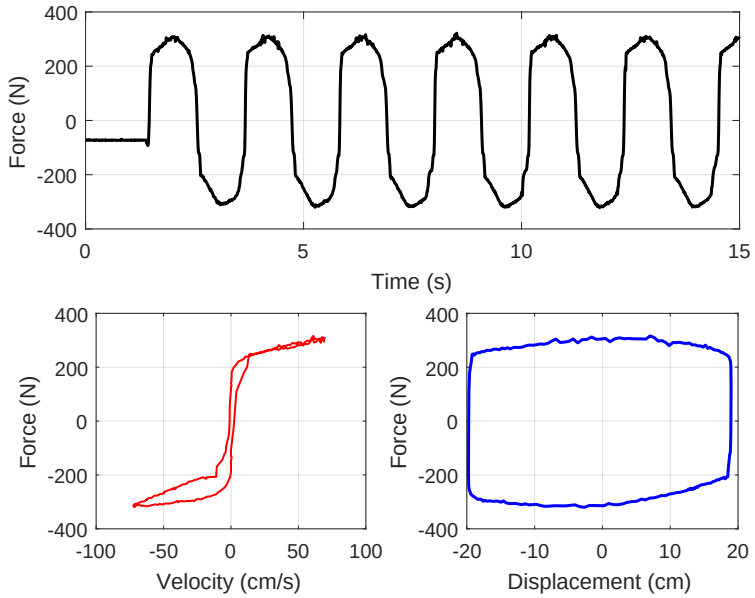

Figure 4.2: Response of the MR damper model with $0.88\,V$.

Table 4.3: MR damper experimental evaluation. Experiments with voltage of $0.88\,V$.

Displacement (mm)	**Frequency** (Hz)	k_x $(N.s.mm^{-1})$	k_w (N)	ρ (mm^{-1})
38.77	0.4629	1.0640	236.6360	19.4264
35.89	0.4808	1.2243	219.6317	20.0219
32.86	0.4926	1.2442	224.2597	19.1666
26.90	0.5525	1.5333	200.2333	18.9063
29.77	0.5236	1.2591	210.3341	20.8018
19.71	0.6250	0.8947	225.6158	19.5472
24.68	0.5682	1.4875	197.9437	22.2421
22.10	0.5988	1.3647	203.5118	19.5472
17.57	0.6667	1.4000	193.9000	22.6884
22.41	0.8474	1.6689	184.5655	21.9603

Table 4.4: MR damper experimental evaluation. Experiments with voltage of $1.98\,V$.

Displacement (mm)	**Frequency** (Hz)	k_x $(N.s.mm^{-1})$	k_w (N)	ρ (mm^{-1})
19.18	0.8378	2.2698	412.4876	10.950
17.98	0.8671	2.0742	403.5954	12.947
16.55	0.9010	2.4235	393.5434	11.074
15.10	0.9438	2.4632	381.0273	11.887
13.43	0.9688	2.1390	398.5763	10.174
12.36	1.0190	3.0239	360.9492	18.264
11.09	1.0520	2.7250	366.7000	20.523
10.03	1.1080	2.8490	357.6377	11.204
8.695	1.1710	2.7943	359.0914	10.802
7.625	1.2050	3.0000	372.5011	17.482

Table 4.5: MR damper experimental evaluation. Experiments with voltage of $3.21\,V$.

Displacement (mm)	**Frequency** (Hz)	k_x $(N.s.mm^{-1})$	k_w (N)	ρ (mm^{-1})
16.95	0.8428	4.6254	614.1636	5.4859
16.21	0.8697	4.8262	599.2934	6.3070
14.88	0.9089	4.7860	577.3067	6.9374
13.71	0.9329	4.9830	569.4712	9.5121
12.52	0.9701	5.1231	540.4077	7.7501
9.385	1.0090	6.0500	568.8500	8.4001
8.270	1.0670	5.9850	525.7800	7.2289
7.370	1.0970	4.8733	573.8467	13.573
6.300	1.1500	6.9524	526.6905	6.9902
5.135	1.2070	7.5217	524.8435	6.0923

4.4 MODEL VALIDATION

The Dahl model with the polynomials in (4.6)–(4.8) produced an error of 21.71%. This value is compatible with the error obtained in (AGUIRRE et al., 2010a) which was 22%.

Figure 4.3 indicates the similarity between the force obtained experimentally and the force calculated by the Dahl model. The data shown in this figure was collected under a voltage of $0.88\,V$ applied to the damper, using a frequency of $0.8474\,Hz$, which resulted in a maximal displacement of $23.5\,mm$. The Figure 4.4 shows the corresponding hysteresis curve.

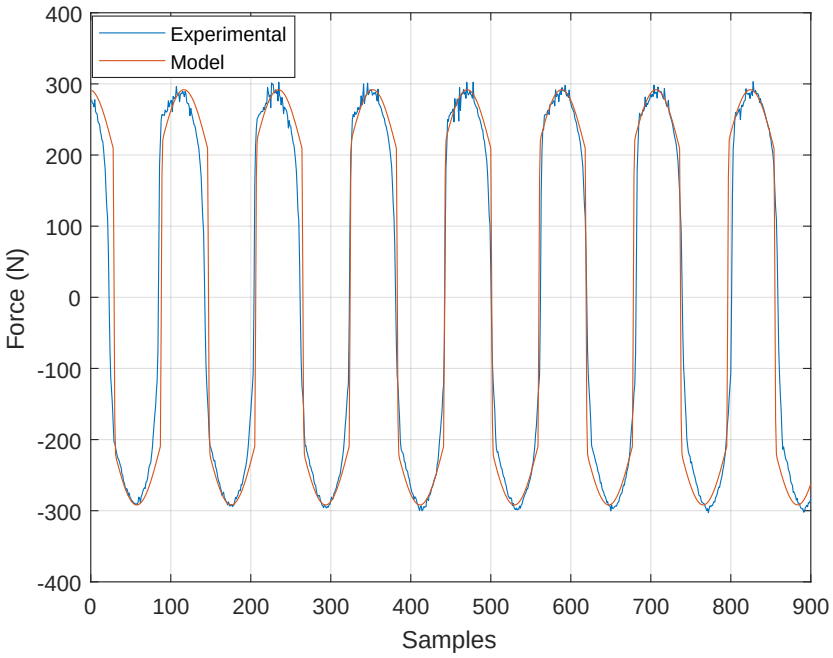

Figure 4.3: Force in the MR damper: data from simulation and experiment. Sample rate used of 0.01 Sa/s.

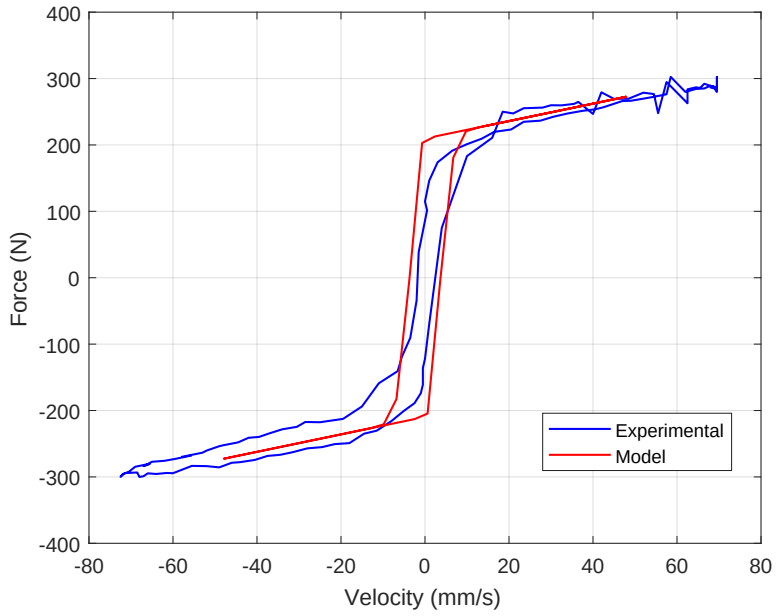

Figure 4.4: Hysteresis curves: data from simulation and experiment.

5 MAGNETORHEOLOGICAL DAMPERS IN STRUCTURES SUBJECT TO EARTHQUAKES

This section presents an application of magnetorheological (MR) dampers in structures. We indicate how MR dampers connected in buildings can mitigate the damages caused by earthquakes. For this purpose, we present simulation-based data only. We link the Dahl model representing an MR damper with a system representing a two-store building. This connection allowed us to obtain an extended model able to simulate a two-store structure with an MR damper attached to its first floor. The building model was then simulated with the El-Centro earthquake (1940), Figure 5.1. The building model was simulated in two scenarios. In the first scenario, the earthquake acts on the building with no MR damper. In the second scenario, the MR damper is included in the building structure. Simulated data indicate the benefits of MR dampers for structures.

5.1 INTRODUCTION

It is usual to see building structures collapse due to earthquakes, natural events that cause death and substantial economic losses (DANIELL et al., 2011), (PARKER; STEENKAMP, 2012).

To make these structures safer for their occupants, researchers have developed techniques such as foundation soil preparation (NANDA et al., 2018), base isolators (OZBULUT; HURLEBAUS, 2011), tuned mass dampers (GARRIDO; SARRAZIN, 2017) and semi-active dampers (XU; LI, 2011). Magnetorheological dampers have been used to mitigate the impacts of earthquakes as well, mainly due to the damper's stability and simple configuration (XU et al., 2019).

To analyze the effects of vibration in structures, the authors of (DYKE et al., 1999) conducted a shaking-table test on a three-story steel frame, and they have shown the effectiveness of the Clipped-Optimal control algorithm for an MR damper attached

b

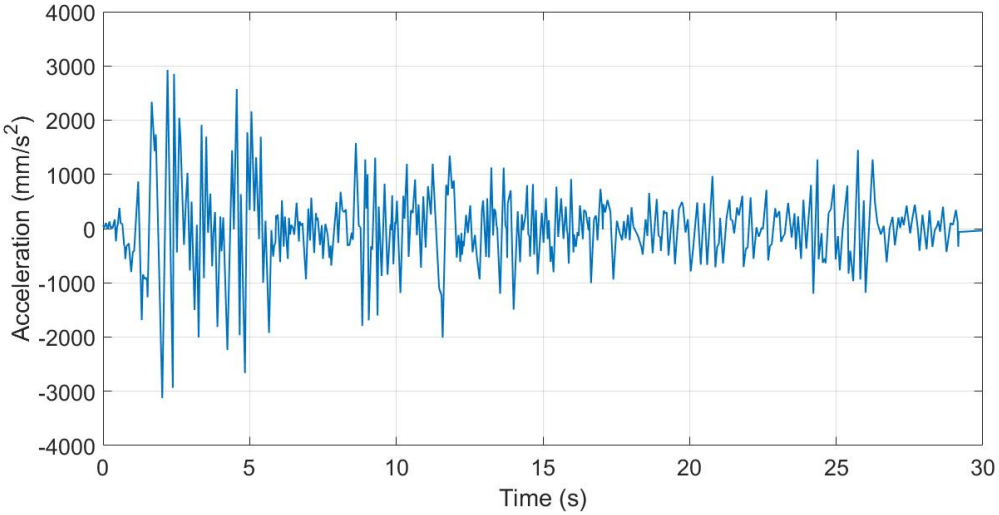

Figure 5.1: El-Centro earthquake.

to the building's first floor. The authors of (SAHASRABUDHE; NAGARAJAIAH, 2005) performed a shaking table test on a two-story steel model to examine whether controllable MR dampers can reduce base displacements without further increasing the superstructure response. (LI et al., 2013) carried out a shaking table test on a three-story steel-concrete structure to investigate the feasibility of MR dampers in seismic control. (DAMCI; SEKERCI, 2018) developed a low-cost single-axis shake table based on Arduino for testing scaled structure models. More recently, (XU et al., 2019) conducted a shaking table test on a three-story steel structure to analyze a piecewise control algorithm that used feedback signals from the story drift and ground excitation acceleration. These investigations together indicate that MR dampers can mitigate the effects of vibrations in buildings. This monograph contributes to this discussion, as described next.

This section presents data from simulation only. The simulation data confirm the benefits of using MR dampers in buildings. The simulation was designed to replicate the behavior of a two-story structure when it is subjected to earthquakes. Three scenarios were considered: (Case 1) Structure without MR damper; (Case 2) Structure with MR damper without voltage (i.e., 0V); and (Case 3) Structure with MR damper regulated at 3.6V, maximum voltage accepted by the MR damper.

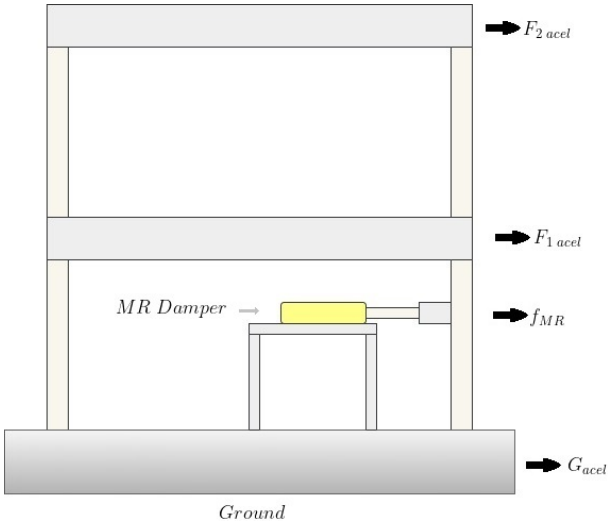

Figure 5.2: Diagram of MR damper implementation.

5.2 MODEL AND SIMULATION

The first step in finding the model of the two-story building attached to an MR damper was to obtain a standalone model capable of describing the non-linear (hysteresis) behavior of the MR damper. This task was accomplished in Section 4. The second step consists of using the two-story building model available in (AGUIRRE et al., 2010b), which reads as

$$M\ddot{Q}+C\dot{Q}+KQ=-MT\ddot{x}_g+\Lambda f, \tag{5.1}$$

where x_g is the acceleration of the ground with respect to the structure, f corresponds to the force exerted by the MR damper, $Q=[x_1,x_2,...,x_n]^T$, $\dot{Q}=[\dot{x}_1,\dot{x}_2,...,\dot{x}_n]^T$ and $\ddot{Q}=[\ddot{x}_1,\ddot{x}_2,...,\ddot{x}_n]^T$, correspond to the displacement, velocity and acceleration relative to the building base, respectively and n denotes the number of stories in the building.

The mass of the structure is represented by the matrix M (Ns^2/mm), the stifness by the matrix K (N/mm), and the damping by the matrix C (Ns/mm). The following values were taken from (AGUIRRE et al., 2010b) and describe the physical properties of the two-store structure.

$$M=\begin{bmatrix}0.1458 & 0\\ 0 & 0.1458\end{bmatrix} \quad K=\begin{bmatrix}131.1 & -65.55\\ -65.55 & 65.55\end{bmatrix} \quad C=\begin{bmatrix}0.2489 & -0.0830\\ -0.0830 & 0.1659\end{bmatrix} \tag{5.2}$$

The element $T = [1,1]^T$ means that the external excitation coming from the ground affects the entire structure. The element $\Lambda = [-1,0]^T$ means the damper is positioned on the first floor.

Equation (5.1) can be represented in the state-space form as

$$\dot{X} = A_s X + B_s f + E_s \ddot{x}_g \tag{5.3}$$

$$y = C_y X + D_y f \tag{5.4}$$

$$A_s = \begin{bmatrix} 0_{n\times n} & I_{n\times n} \\ -M^{-1}K & -M^{-1}C \end{bmatrix} \quad B_s = \begin{bmatrix} 0_{n\times 1} \\ M^{-1}\Lambda \end{bmatrix} \quad E_s = \begin{bmatrix} 0_{n\times 1} \\ -T \end{bmatrix} \tag{5.5}$$

$$C_y = \begin{bmatrix} -M^{-1}K & -M^{-1}C \end{bmatrix} \quad D_y = \begin{bmatrix} -M^{-1}\Lambda \end{bmatrix} \tag{5.6}$$

where $X = [x_1, x_2, ..., x_n, \dot{x}_1, \dot{x}_2, ..., \dot{x}_n]^T$ denotes the state vector, and the variables x_i, $\dot{x}_i$ and $\ddot{x}_i$ represent the displacement, velocity and acceleration of the i-th floor. The output vector y stands for the absolute accelerations of all floors.

The simulations were carried out with real data taken from the 1940 El-Centro earthquake in California, see Figure 5.1. The system in (5.3)–(5.6) was coded in MATLAB/Simulink and can be seen in Figure 5.3.

Data from the simulations are depicted in Figure 5.4. As can be seen, for the three distinct scenarios, the behavior of the building structure changes dramatically. For instance, in the case with no damper (Case 1), the first floor reached the peak displacement of $223.1413\,mm$, which in practice represents a danger of collapse of the overall structure.

When we consider the MR damper, there is a reduction of 7.01% in the maximum displacement ($216.8413\,mm$ for Case 2), and there is a reduction of 13.66% ($201.5243\,mm$ for Case 3).

In summary, the best case for the structure's safety is when the MR damper is active with voltage. As the simulations suggest, MR dampers can mitigate the effects of earthquakes upon building structures.

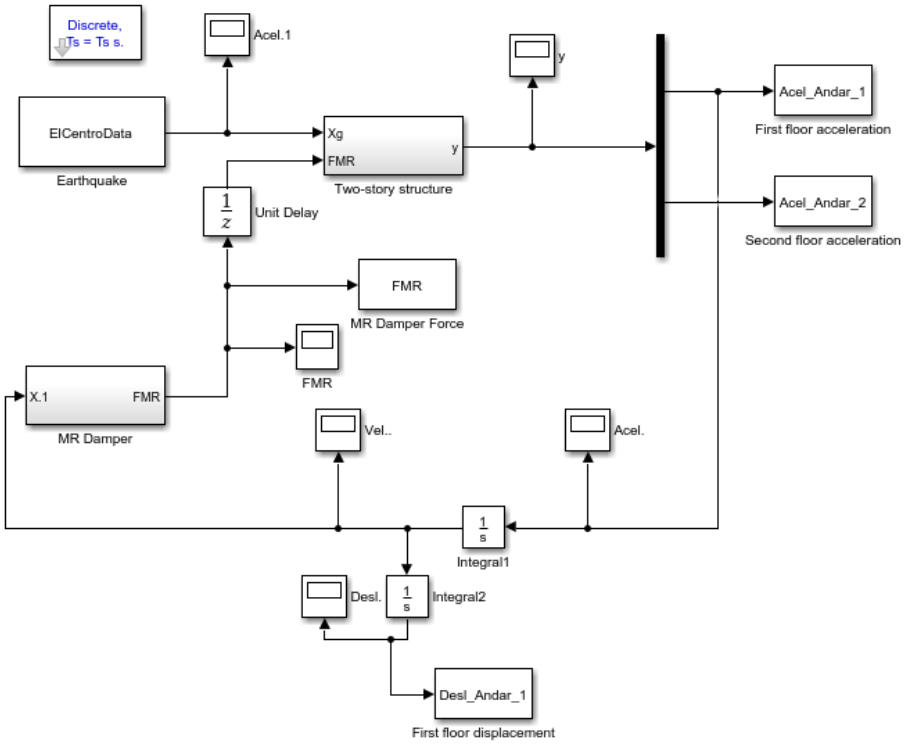

Figure 5.3: System coded in Simulink.

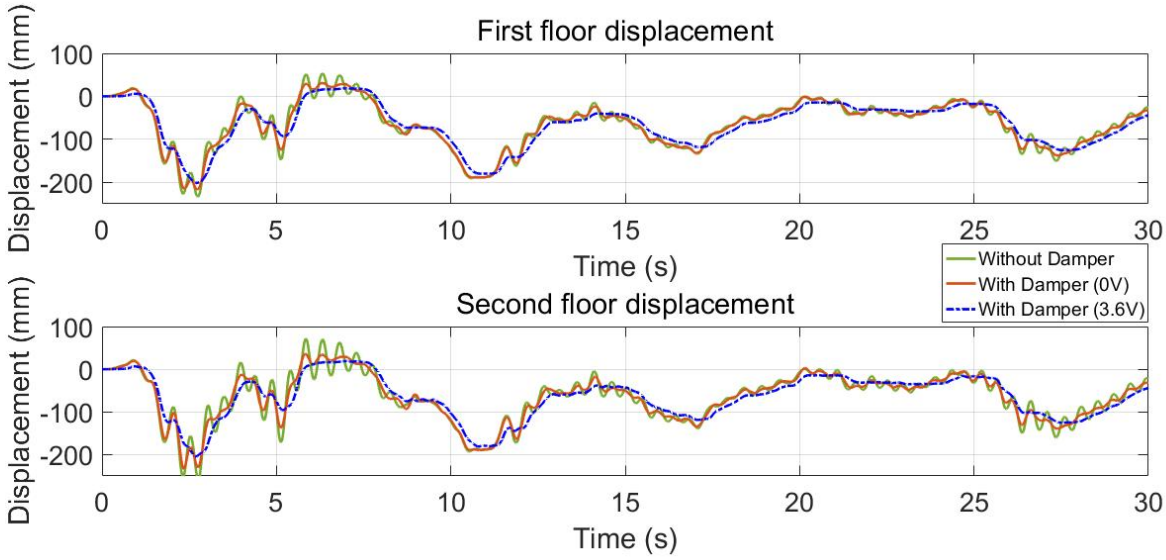

Figure 5.4: Comparison between the scenarios.

6 CONCLUSÃO

Os amortecedores MR são dispositivos úteis para diversas aplicações, por exemplo, em estruturas para mitigar vibrações. O uso de amortecedores MR traz consigo vários desafios, incluindo a representação correta de seu comportamento para fins de projeto. Sabe-se que tais amortecedores possuem histerese, fenômeno não linear de difícil tratamento.

Para melhor compreender o comportamento dinâmico dos amortecedores MR, o autor desta dissertação propõe o desenvolvimento de uma plataforma experimental para testes de amortecedor magneto-reológico. Foi construída uma plataforma de ensaios dinâmicos, contendo um amortecedor MR. Este projeto incluiu instrumentação completa para o comando do sinal de entrada, deslocamento da mesa e medição da força gerada pelo amortecedor MR. A plataforma de teste foi fabricada na UTFPR e possibilitou a realização de testes que consistem em excitar o sistema com diferentes entradas, deslocamentos e frequências.

O autor apresentou um modelo para descrever o comportamento de histerese do amortecedor magneto-reológico. Após obter o modelo, este foi usado para simular uma estrutura de edifício, em escala reduzida sujeita a um terremoto. A proposta foi analisar o impacto do amortecedor MR no comportamento da estrutura avaliando o deslocamento dos andares.

Três casos foram testados. O primeiro apenas a estrutura foi exposta ao terremoto, no segundo caso o amortecedor MR foi adicionado à estrutura, mas não foi aplicado tensão, e no último foi aplicado uma tensão elétrica de $3,6\,V$ no amortecedor MR conectado à estrutura. Os resultados da simulação indicam que o amortecedor MR foi capaz de reduzir o deslocamento da estrutura em todos os testes em que foi empregado.

Em resumo, a simulação indica que amortecedor MR pode ser usado em estruturas sujeitas a terremotos, de modo a mitigar os possíveis efeitos destrutivos causados

pelos terremotos.

APPENDIX A – COMPONENTS

The damper used in this study is manufactured by Lord Corporation model RD-8041-1, its specifications are in table A.1.

Table A.1: Magnetorheological damper properties.

Stroke	74 *mm*
Extended Length	248 *mm*
Body Diameter	42.1 *mm*
Shaft Diameter	10 *mm*
Tensile Strength	8896 *N*
Damper Forces (Peak to Peak)	
5 cm/sec @ 1 A	$> 2447\ N$
20 cm/sec @ 0 A	$< 667\ N$
Operating Temperature	71 $^{\circ}C$

The workbench uses a ball screw linear actuator manufatured by GlideForce, specification on table A.2, for system excitation and is controlled using a Arduino Uno microcontroller and a IBT-3 Motor Drive Module, specification on table A.3.

Table A.2: Ball screw linear actuator properties.

Stroke	457 mm
Extended Length	1194 mm
Gear Ratio	$20:01$
Max Load	4500 N
Speed/No Load	16.8 mm/sec
Speed/Max Load	14.3 mm/sec
Current /No Load	2.4 A
Current /Max Load	13.2 A

Table A.3: IBT-3 Motor Drive Module properties.

Maximum current	50 A
Maximum PWM frequency	200 KHz
Power supply voltage	$5\,V - 15\,V$

For force and displacement measurement, a load cell model ZSL manufatured by IWM, specification on table A.4, and a linear encoder model KA-300 manufatured by Sino, specification on table A.5, are used.

Table A.4: Load cell properties.

Maximum workload	500 kg
Sensitivity	1.955 mV/V
Linearity	$< 0.02\,\%$
Hysteresis	$< 0.02\,\%$
Safe load limit	150 %

Table A.5: Linear encoder properties.

Scaling Distance	0.02 mm (50 $lines/mm$)
Resolution	5 μm
Precision	± 5 μm
Measuring range	370 mm
Moving speed	60 m/min
Power supply	± 5 $V \pm 5$ V 80 mA
Working Temperature	0 to 45$^{\circ}C$

The generated data is extracted using a National Instruments acquisition board model NI PCI-6221.

REFERÊNCIAS

AGUIRRE, N. et al. Modeling and identification of a small scale magnetorheological damper. **IFAC Proceedings Volumes**, v. 43, n. 10, p. 19–24, 2010.

AGUIRRE, N. et al. Viscous + Dahl Model for Mr Dampers Characterization : a Real Time Hybrid Test (RTHT) Validation. **14th European Conference on Earthquake Engineering 2010**, n. May, p. 822, 2010.

AGUIRRE, N. et al. Parametric identification of the Dahl model for large scale MR dampers. **Structural Control and Health Monitoring**, v. 23, p. 742–760, 2012.

ANDERSON, E.; HAGOOD, N.; GOODLIFFE, J. Self-sensing piezoelectric actuation - analysis and application to controlled structures. 02 1992.

BOUC, R. Modèle mathématique d'hystérésis. Acustica, 1971.

CARLSON, J. D.; JOLLY, M. R. MR fluid, foam and elastomer devices. **Mechatronics**, v. 10, p. 555–569, 2000.

CHEN, Z.; LAM, K. H.; NI, Y. Enhanced damping for bridge cables using a self-sensing mr damper. **Smart Materials and Structures**, v. 25, p. 085019, 08 2016.

DAHL, P. R. A solid friction model. The Aerospace Corporation, 05 1968.

DAMCI, E.; SEKERCI, C. Development of a low-cost single-axis shake table based on arduino. **Experimental Techniques**, v. 43, p. 179–198, 2018.

DANIELL, J. et al. The catdat damaging earthquakes database. **Natural Hazards and Earth System Sciences - NAT HAZARDS EARTH SYST SCI**, v. 11, p. 2235–2251, 08 2011.

DO, P.; CHOI, S.-M.; CHOI, S.-B. A new adaptive hybrid controller for vibration control of a vehicle seat suspension featuring mr damper. **Journal of Vibration and Control**, v. 23, 02 2016.

DUTTA, S.; CHOI, S.-B. Control of a shimmy vibration in vehicle steering system using a magneto-rheological damper. **Journal of Vibration and Control**, v. 24, p. 797–807, 2018.

DYKE, S. et al. An experimental study of mr dampers for seismic protection. **Smart Materials and Structures**, v. 7, p. 693, 01 1999.

FARAJ, R.; GRACZYKOWSKI, C.; HOLNICKI-SZULC, J. Adaptable pneumatic shock absorber. **Journal of Vibration and Control**, 08 2018.

GAO, F.; LIU, Y.-N.; LIAO, W.-H. Optimal design of a magnetorheological damper used in smart prosthetic knees. **Smart Materials and Structures**, IOP Publishing, v. 26, n. 3, p. 035034, feb 2017.

GARRIDO, B.; SARRAZIN, M. Effectiveness of tuned mass dampers (tmd) for earthquake protection in chilean buildings. In: . [S.l.: s.n.], 2017.

GE, P.; JOUANEH, M. Modeling hysteresis in piezoceramic actuators. **Precision Engineering**, v. 17, n. 3, p. 211–221, 1995.

IKHOUANE, F.; RODELLAR, J. **Systems with Hysteresis: Analysis, Identification and Control Using the Bouc-Wen Model**. [S.l.: s.n.], 2007.

INMAN, D. J.; CARNEIRO, S. H. S. 7. smart structures, structural health monitoring and crack detection. In: _____. **Research Directions in Distributed Parameter Systems**. [S.l.: s.n.], 2020. p. 169–186.

ISMAIL, M.; IKHOUANE, F.; RODELLAR, J. The hysteresis Bouc-Wen model, a survey. **Archives of Computational Methods in Engineering**, v. 16, n. 2, p. 161–188, 2009.

JOLLY, M. R.; BENDER, J. W.; CARLSON, J. D. Properties and Applications of Commercial Magnetorheological Fluids. **Frattura ed Integrita Strutturale**, v. 23, p. 57–61, 2012. ISSN 19718993.

KONIECZNY, J. et al. Laboratory research of the controllable hydraulic damper. **Engineering Transactions**, v. 54, p. 203–221, 01 2006.

LI, Z.-X. et al. Experimental studies on nonlinear seismic control of a steel–concrete hybrid structure using mr dampers. **Engineering Structures**, v. 49, p. 248–263, 04 2013.

LIMA, A. S. D. **Identificação experimental de um sistema magneto-reológico**. Tese (Doutorado) — COPPE-UFRJ, 2011.

MENG, F. et al. Modeling and experimental verification of a squeeze mode magnetorheological damper using a novel hysteresis model. **Proceedings of the Institution of Mechanical Engineers, Part C: Journal of Mechanical Engineering Science**, v. 233, 04 2019.

NANDA, R. P.; DUTTA, H. A. K. S.; MAJUMDER, S. Seismic Protection of Buildings by Rubber-Soil Mixture as Foundation Isolation. **Reserve Bank of New Zealand Bulletin**, 2018.

NOËL, J. P. et al. Hysteresis identification using nonlinear state-space models. **Conference Proceedings of the Society for Experimental Mechanics Series**, v. 1, p. 323–338, 2016. ISSN 21915652.

OZBULUT, O.; HURLEBAUS, S. Optimal design of superelastic-friction base isolator for seismic protection of highway bridges against near-fault earthquakes. **Earthquake Engineering and Structural Dynamics**, v. 40, p. 273 – 291, 03 2011.

PARKER, M.; STEENKAMP, D. The economic impact of the Canterbury earthquakes. **Reserve Bank of New Zealand Bulletin**, v. 75, p. 13–25, September 2012.

PIATKOWSKI, T. Dahl and lugre dynamic friction models — the analysis of selected properties. **Mechanism and Machine Theory**, v. 73, p. 91–100, 03 2014.

PONS, J. L. **Emerging Actuator technologies: A Micromechatronics Approach**. [S.l.: s.n.], 2005.

ROSSI, A. et al. A review on parametric dynamic models of magnetorheological dampers and their characterization methods. **J. Intell. Mater. Syst. Struct.**, v. 7, n. 2, 1999.

SAHASRABUDHE, S.; NAGARAJAIAH, S. Experimental study of sliding base-isolated buildings with magnetorheological dampers in near-fault earthquakes. **Journal of Structural Engineering-Asce**, v. 131, p. 1025–1034, 07 2005.

SALAPAKA, S. et al. High bandwidth nano-positioner: A robust control approach. **Review of Scientific Instruments**, v. 73, 09 2002.

SARNO, R. L.; FRANKE, M. E. Suppression of flow-induced pressure oscillations in cavities. **Journal of Aircraft**, v. 31, n. 1, p. 90–96, 1994.

SEID, S.; SUJATHA, C.; SRINIVASAN, S. Optimal design of an mr damper valve for prosthetic knee application. **Journal of Mechanical Science and Technology**, v. 32, p. 2959–2965, 06 2018.

SPENCER, J. B. F. et al. Phenomenological model for magnetorheological dampers. **J. Engineering Mechanics**, American Society of Civil Engineers, v. 123, n. 3, p. 230–238, 1997.

STUTZ, L. T. **Síntese e Análise de uma Suspensão Semi-ativa Magneto Reológica Baseada na Abordagem de Controle com Estrutura Variável**. 181 p. Tese (Doutorado) — COPPE-UFRJ, 2005.

VICENTE, J.; KLINGENBERG, D. J.; HIDALGO-ALVAREZ, R. Magnetorheological fluids: A review. **Soft Matter**, v. 7, n. 8, p. 3701–3710, 2011.

WEN, Y. Method for random vibration of hysteretic systems. J Eng Mech Div 102(EM2):246–263, 1976.

XU, L.-H.; LI, Z.-X. Model predictive control strategies for protection of structures during earthquakes. **Structural Engineering and Mechanics**, v. 40, 10 2011.

XU, Z.-D. et al. Shaking table tests of magnetorheological damped frame to mitigate the response under real-time online control. **Smart Materials and Structures**, v. 28, 09 2019.

YANG, G. et al. Large-scale MR fluid dampers: Modeling and dynamic performance considerations. **Eng. Struct.**, v. 24, p. 309–323, 03 2002.

YARALI, E. et al. Mathematical modeling and experimental evaluation of a prototype double-tube magnetorheological damper. **SN Applied Sciences**, v. 1, 09 2019.

ZAMANI, A. A. et al. Modeling of a magneto-rheological damper: An improved multi-state-dependent parameter estimation approach. **Journal of Intelligent Material Systems and Structures**, v. 30, 03 2019.

ZAPATEIRO, M. et al. Real time hybrid testing of semiactive control strategies for vibration reduction in a structure with mr damper. **Structural Control and Health Monitoring**, v. 17, p. 427 – 451, 01 2009.